HHS Public Access

Author manuscript

ACS Nano. Author manuscript; available in PMC 2017 January 10.

Published in final edited form as:

ACS Nano. 2015 November 24; 9(11): 10758–10768. doi:10.1021/acsnano.5b05061.

Modulatory Role of Surface Coating of Superparamagnetic Iron Oxide Nanoworms in Complement Opsonization and Leukocyte Uptake

Swetha Inturi[†,#], **Guankui Wang**[†,#], **Fangfang Chen**[‡], **Nirmal K. Banda**[§], **V. Michael Holers**[§], **LinPing Wu**[||], **Seyed Moein Moghimi**[||,⊥], and **Dmitri Simberg**[†,*]

[†]The Skaggs School of Pharmacy and Pharmaceutical Sciences, University of Colorado Anschutz Medical Campus, 12850 East Montview Blvd., Aurora, Colorado 80045, United States

[‡]Department of Gastrointestinal Surgery, China-Japan Union Hospital, Jilin University, 126 Xiantai Street, Changchun, Jilin 130033, China

[§]The Division of Rheumatology, School of Medicine, University of Colorado Anschutz Medical Campus, 1775 Aurora Court, Aurora, Colorado 80045, United States

[||]Nanomedicine Laboratory, Centre for Pharmaceutical Nanotechnology and Nanotoxicology, Department of Pharmacy, Faculty of Health and Medical Sciences, Universitetsparken 2, University of Copenhagen, DK-2100 Copenhagen Ø, Denmark

[⊥]NanoScience Centre, University of Copenhagen, DK-2100 Copenhagen Ø, Denmark

Abstract

Notwithstanding rapid advances of nanotechnology in diagnostic imaging and drug delivery, the engineered nanocarriers still exhibit substantial lack of hemocompatibility. Thus, when injected systemically, nanoparticles are avidly recognized by blood leukocytes and platelets, but the mechanisms of immune recognition are not well understood and strategies to mitigate these phenomena remain underexplored. Using superparamagnetic dextran iron oxide (SPIO) nanoworms (NWs) we demonstrate an efficient and predominantly complement-dependent uptake by mouse lymphocytes, neutrophils and monocytes from normal and tumor bearing mice *in vitro*. Following intravenous injection into wild type mice, blood leukocytes as well as platelets became magnetically labeled, while the labeling was decreased by 95% in complement C3-deficient mice. Using blood cells from healthy and cancer patient donors, we demonstrated that neutrophils, monocytes, lymphocytes and eosinophils took up SPIO NWs, and the uptake was prevented by EDTA (a general complement inhibitor) and by antiproperdin antibody (an inhibitor of the alternative pathway of the complement system). Cross-linking and hydrogelation of SPIO NWs surface by epichlorohydrin decreased C3 opsonization in mouse serum, and consequently reduced the uptake by mouse leukocytes by more than 70% *in vivo*. Remarkably, the cross-linked particles

[*]Address correspondence to: dmitri.simberg@ucdenver.edu.

[#]S.I. and G.W. contributed equally.

Conflict of Interest: The authors declare no competing financial interest.

Supporting Information Available: The Supporting Information is available free of charge on the ACS Publications website at DOI: 10.1021/acsnano.5b05061.

Leukocyte quantification by nuclear staining (images) and by flow cytometry. (PDF)

did not show a decrease in C3 opsonization in human serum, but showed a significant decrease (over 60%) of the uptake by human leukocytes. The residual uptake of cross-linked nanoparticles was completely blocked by EDTA. These findings demonstrate species differences in complement-mediated nanoparticle recognition and uptake by leukocytes, and further show that human hemocompatibility could be improved by inhibitors of complement alternative pathway and by nanoparticle surface coating. These results provide important insights into the mechanisms of hemocompatibility of nanomedicines.

Graphical abstract

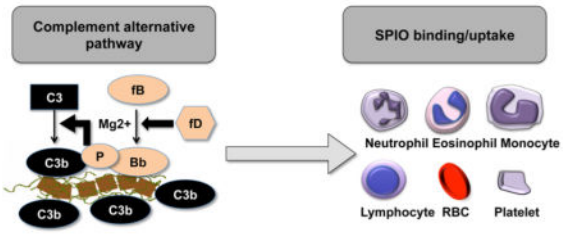

Keywords

nanoworms; leukocytes; immunity; iron oxide; leukocyte; complement; alternative pathway

Nanomedicine holds great promise for medical imaging and site-specific drug delivery with engineered nanoparticles (NPs);[1,2] however, intravenously injected NPs encounter many biological barriers before they can reach the desired targets within the vasculature or beyond. Among these, elements of the innate immune system, and notably blood leukocytes and tissue macrophages, are key players intercepting blood-borne nanoparticles and pathogens.[3–5] The propensity of macrophages and related immune cells to rapidly recognize and sequester nanoparticles can offer an unprecedented opportunity to selectively delivery of antigens and therapeutic agents to such cells for imaging and therapy. On the other hand, rapidly intercepting and eliminating nanomedicines is problematic if the intended target site for therapeutic intervention lies elsewhere. Accordingly, this may decrease specificity of targeting and imaging, provoking untoward responses and inducing off-target toxicities.[7,8]

The complement system is a critical component of the innate immunity accounting for about 5% of globulins in serum and is responsible for recognizing, eliminating, and destroying pathogens.[4] Activation of the complement on the surface of a foreign agent proceeds *via* the classical pathway (CP), lectin pathway (LP) or alternative pathway (AP), and converges to form highly reactive thioester C3b that covalently binds to reactive groups (*e.g.*, amines and hydroxyls) on the surface of the activator. Opsonization by C3b triggers particle recognition by phagocytic cells through their complement receptors,[3,5] whereas soluble cleavage byproducts C3a and C5a are potent anaphylatoxins and proinflammatory molecules with low nanomolar affinity for their corresponding receptors.[6] Accordingly, complement activation plays an important role in nanoparticle clearance and adverse immune reactions.[7,8] Numerous nanoplatforms have been shown to activate complement *in vitro* and *in vivo*.[8–23] Uncontrolled complement activation in human patients may contribute to infusion-related

reactions, and this has been demonstrated in the case of various clinically approved nanopharmaceuticals (Doxil, Feridex, Taxol).

Superparamagnetic iron oxide (SPIO) was one of the first clinically approved nanodiagnostics employed in magnetic resonance imaging (MRI) contrast agent. SPIO is also actively being explored as part of complex nanoassemblies and multifunctional theranostic nanomedicines.[24] SPIO consists of negatively charged magnetite-maghemite (Fe_3O_4 and γ-Fe_2O_3) crystals coated with a polysaccharide polymer (usually dextran or carboxymethyl dextran). Others[25] and our group[26,27] reported synthesis and characterization of elongated worm-like SPIO (dubbed nanoworms) made from 20 kDa dextran chains. Recently, we reported that SPIO NWs potently activate complement in mouse and human sera leading to the deposition of C3b/iC3b on the nanoparticle surface.[28] In mice, SPIO NWs activate the lectin pathway due to the initial binding of mannose binding lectin (MBL-A/C) and MBL-associated serine protease MASP-2. In humans, the lectin pathway is also activated, but the majority of activation comes from a direct surface-mediated increase of the alternative pathway turnover.[28]

Here we used SPIO NWs to study the role of complement in the uptake by leukocytes of mouse and the human blood. The unique advantage of magnetic nanoparticles for such experiments is the easy magnetic isolation and enrichment of cells, thus facilitating mechanistic studies. Albeit the uptake of nanoparticles by blood leukocytes has been reported before,[29–33] the role of complement in the leukocyte uptake of iron oxides has not been conclusively demonstrated.

RESULTS

We prepared non-cross-linked 20 kDa dextran-coated SPIO NWs by a modified Molday precipitation method[34] as described by us earlier.[26] The particles appeared as worm-like structures by TEM (Figure 1A), with multiple electron-dense magnetite-maghemite cores per nanoparticle embedded in dextran chains and a hydrodynamic diameter of 111.4 ± 28 nm. SPIO NWs were preincubated in fresh mouse serum for 15 min and washed by ultracentrifugation. C3 was detected on the particles by a dot blot assay (Figure 1B) using an antibody that recognizes a variety of C3 fragments (C3b, iC3b, C3d *etc.*).[28] There was a significant deposition of C3 in wild-type (WT) mouse serum (Figure 1C), but not in $C3^{-/-}$ mouse serum or in serum pretreated with 4 mM EDTA (a general complement inhibitor).

1. *In Vitro* Uptake of SPIO NW by Mouse Leukocytes Is C3 Dependent

For *in vitro* uptake experiments, mouse blood cells were washed in PBS in order to remove excess of heparin, an anticoagulant and complement inhibitor. SPIO NWs was preincubated with serum and then added to the washed mouse blood cells (leukocytes, red blood cells and platelets) obtained from C45/BL5 or BALB/c mice. The cells that bound or internalized SPIO NWs were isolated using a Mini MACS magnetic column (Figure 2A). The isolation sensitivity is high, because SPIO NWs have very high magnetization values,[26] and the magnetic beads are capable of isolating rare cells, for example circulating tumor cells.[35] The eluted cells were concentrated on a slide and stained with antidextran antibody and anti-CD11b antibody (complement receptor 3 (CR3)), and the nuclei were stained with Hoechst.

We used nuclear shape to identify and enumerate the magnetically labeled cells (Figure 2B). Nuclear shape is one of the classical parameters for leukocyte identification,[36] and has been found to be a reliable parameter for leukocyte type classification.[37,38] We verified that nuclear shape classification by microscopy highly correlates with forward scattering-side scattering classification by flow cytometry (Supporting Information). The majority of leukocytes were $CD11b^+$ neutrophils, albeit lymphocytes and monocytes also showed dramatic uptake (Figure 2C,D). In order to test the role of complement in the leukocyte uptake, SPIO NWs were preincubated with sera from $C3^{-/-}$ mice before adding to the washed blood cells. As a result, the number of magnetically labeled neutrophils decreased by 90%, and the number of monocytes decreased by ~70% (Figure 2C,D).

Since nanoparticles are being actively explored for tumor drug delivery and imaging, we questioned whether SPIO NWs are also taken up by leukocytes from tumor-bearing mice, and whether the uptake is complement-dependent. We used 4T1 breast cancer allograft model in BALB/c mice, which metastasizes within 1 week postinjection.[39] Mice with 5–10 mm diameter tumors had 3–5 times more neutrophils compared to nontumor-bearing mice, and correspondingly there were 3 times more $CD11^+$ neutrophils that took up SPIO NWs (Figure 2E,F). The number of magnetically labeled leukocytes decreased by 95% when SPIO NW was preincubated in $C3^{-/-}$ serum (Figure 2E,F), confirming that leukocytes in tumor mice take up SPIO NWs in a complement-dependent manner.

2. SPIO NWs Are Internalized after Intravenous Bolus by Mouse Leukocytes, and the Uptake Is C3 Dependent

In order to determine the uptake of SPIO NWs by leukocytes *in vivo*, nanoparticles were injected as a 0.1 mg bolus into normal C57/BL6 mice. Following the injection, we collected heparinized blood at different time points (10 min, 1h and 24 h) and isolated the cells as outlined in Figure 3A. At 10 min postinjection, a significant proportion of neutrophils, lymphocytes and monocytes were magnetically labeled, albeit the ratio between neutrophils and lymphocytes varied between experiments. At 1h postinjection, as many as 16.8 ± 4.9% (n = 3 mice) of total blood leukocytes were magnetically labeled. Results of a representative experiment (Figure 3B) show that the majority of magnetically isolated cells at 1h postinjection were neutrophils. The number of magnetically labeled leukocytes in circulation decreased 5-fold at 24 h postinjection. Parallel injection experiments in $C3^{-/-}$ mice (C57/BL6J background) showed that there were 95% less magnetically labeled neutrophils and lymphocytes compared to normal C57/BL6 mice at 1h postinjection (Figure 3B).

Since the number of circulating magnetically labeled leukocytes dropped dramatically at 24 h, we questioned whether SPIO NWs uptake accelerated the clearance of leukocytes. The total leukocyte count in blood did not change after the injection (not shown). We isolated leukocytes from normal C45/BL6 mice and prelabeled them with carboxyfluorescein succinimidyl ester (CFSE, Figure 4A). CFSE effectively and irreversibly labels the cytoplasm of cells and can be used for *in vivo* cell tracking and proliferation.[40] The CFSE labeled leukocytes were incubated with SPIO NWs as described in Figure 2A and the magnetically labeled leukocytes were isolated using a MACS column and injected into another mouse (0.3–0.5 million cells/animal). For a control, CFSE labeled leukocytes that

were not trapped in the column were injected into a control mouse. In both groups, the cells did not form clusters before the injection. According to Figure 4B, CFSE-labeled leukocytes were present in blood at 10 and 60 min postinjection in both groups. At 24 h postinjection, CFSE-labeled leukocytes in both groups were absent from peripheral blood. At 24 h post injection, CFSE labeled leukocytes were found in the spleen, but not in the liver or kidney (Figure 4C). Inspection of lungs, lymph nodes or bone marrow did not reveal CFSE labeled cells (not shown). Because of the short duration of this experiment, the numbers of cells in organs reflect true distribution rather than cell proliferation. We conclude that the observed evacuation of magnetically labeled leukocytes from blood (Figure 3B) is the part of normal process of leukocyte recirculation.[40,41]

In addition to leukocytes, we observed that mouse platelets also became magnetically labeled *in vitro* and *in vivo* (Figure 5A). No platelets were captured by MACS column from control blood (not shown). There was a significant drop in the number of magnetically labeled platelets in $C3^{-/-}$ serum *in vitro* and in $C3^{-/-}$ mice *in vivo* (Figure 5B,C; E,F). Interestingly, a significant proportion of platelets were associated with leukocytes in wild-type experiments *in vitro* and *in vivo*, and much less association was observed in $C3^{-/-}$ experiments (Figure 5A,D).

3. The Uptake of SPIO NWs by Human Leukocytes is C3 Dependent

Next, we investigated the role of complement in human leukocyte uptake. We used washed blood leukocytes obtained from healthy male and female donors. The human leukocyte uptake studies, with the exception of the conditions of incubation of SPIO NWs with serum (see Materials and Methods), were performed exactly as mouse experiments. According to Figure 6A, neutrophils, monocytes, lymphocytes and eosinophils became magnetically labeled after incubation with SPIO NWs *in vitro*. Since there are no C3-deficient human individuals, and commercially available C3-depleted sera often contain additives and complement blockers, we used complement inhibitors in order to inhibit C3 opsonization of SPIO NWs. In humans, SPIO NWs activate the lectin and the classical pathway (in some individuals with antidextran antibodies through the classical pathway), but the alternative pathway is self-sufficient and responsible for the majority of C3 deposition (summarized in Figure 6B).[28] The alternative pathway (AP) requires presence of properdin (factor P), which is present in blood at ~20 μg/mL and stabilizes AP-derived C3 convertases.[42] Human C3 deposition on SPIO NWs (Figure 6C) was decreased by over 95% using 4 mM EDTA (an inhibitor of all complement pathways) and by 70% using antiproperdin (anti-P) antibody (a specific inhibitor of the AP[43]). The number of magnetically labeled cells of all types was decreased as much as 90% in both EDTA-treated serum and anti-P-treated serum (Figure 6D,E). Similar to mouse experiments, neutrophils were highly dependent on C3 opsonization for the uptake, but monocytes, lymphocytes and eosinophils also showed dependency on the complement (Figure 6D,E). In addition to normal healthy donor blood, we also tested the role of complement in the uptake of serum-preincubated SPIO NWs by blood cells from metastatic breast cancer patient. As shown in Figure 6F, there was an efficient uptake by cancer patient's leukocytes and complete blockade by EDTA and antiproperdin antibody.

4. Cross-Linking and Hydrogelation of Dextran Coat Blocks Leukocyte Uptake Independently of Complement Activation

Reaction of dextran hydroxyls with epichlorohydrin leads to hydrogel coated cross-linked nanoworms (CL-NWs, Figure 7A).[26,27,44] Previously we demonstrated that cross-linking blocks the lectin pathway activation in mouse serum and consequently decreases complement C3 opsonization[28] and decreases macrophage recognition in mice.[45] We set out to determine whether cross-linking blocks the leukocyte uptake in mouse and human sera. The cross-linking minimally changed the size of nanoworms (114 nm before and 83 nm after) and did not change the worm-like shape of the nanoparticles (Figure 7B). Cross-linking resulted in a formation of poly(2-hydroxypropyl ether) hydrogel as measured by iodine assay,[26] with 0.6 mg of ethylene oxide per milligram of iron (Figure 7C). There was a significant (70%) decrease in C3 opsonization of CL-NWs in mouse serum compared to non-cross-linked SPIO NWs (Figure 7D). Intravenous injection of CL-NWs into normal C57/BL6 mice showed over 70% decrease in the number of magnetically labeled leukocytes in mouse blood compared to non-cross-linked SPIO NW (Figure 7E,F). In human serum, however, cross-linking did not decrease C3 opsonization of CL-NWs (Figure 7G), likely due to the predominant role of the alternative pathway in human serum.[28] At the same time, incubation with human blood cells from a healthy donor showed 60% decrease (30–70% range for 5 different blood donors, not shown) in the number of magnetically labeled cells after 1h incubation (Figure 7H,I). The C3 opsonization and the residual uptake of CL-NWs by human leukocytes was inhibited by EDTA (Figure 7G,I). These data suggest that cross-linked hydrogel coating partially inhibits the complement-dependent uptake of nanoparticles.

DISCUSSION

This report demonstrates that recognition of iron oxide nanoparticles by leukocytes and platelets is mediated exclusively *via* complement C3 in normal donors and cancer patients, and across different species (mice and humans). SPIO NWs are different from the clinical (now abandoned) SPIO Feridex: the latter was manufactured with 10 kDa dextran, and the particles have a spherical rather than a worm-like shape. Nevertheless, Feridex showed significant complement-related toxicity in clinical use, and the injection of this agent into rats at 20 mg Fe/kg resulted in labeling of 5% of leukocytes *in vivo*.[30] Therefore, we suggest that complement-triggered leukocyte uptake could be relevant to many types of iron oxide-based MRI agents. Numerous other nanoplatforms including gold, polymeric nanoparticles, carbon nanotubes, liposomes and micelles have been shown to activate complement *in vitro* and *in vivo*,[8–23] and it remains to be elucidated whether these nanomaterials are also sequestered by leukocytes *via* complement-mediated mechanisms. We demonstrated that immune uptake of nanoparticles by human leukocytes can be prevented by inhibitors of the alternative pathway of complement (antiproperdin antibody), which could make the complement cascade an attractive target to improve hemocompatibility of nanomaterials. At the same time, we demonstrate that surface cross-linking could be an independent strategy to decrease leukocyte uptake, regardless of the level of complement activation. The strong inhibition of CL-NW uptake by human leukocytes despite C3 opsonization is a counterintuitive result, but is in line with previous observations. Thus, studies using

liposomes bearing PEG 2000 showed that although complement is activated, the steric barrier of PEG is strong enough to prevent the binding of C3 opsonized liposomes to macrophages.[21] Another study demonstrated the lack of correlation between C3 opsonization and long-circulating properties of PEGylated liposomes.[46] The reasons why cross-linked polymer coating renders nanoparticles less recognizable by leukocytes despite C3 opsonization need to be further investigated, but it could be speculated that hydrogel coatings change conformation of surface bound C3 and/or reduces interaction between C3 (C3b and iC3b) and complement receptors due to steric effects.

We still do not know much about the receptors responsible for recognition of complement-opsonized SPIO NWs by leukocytes and platelets. Neutrophils express complement receptors C1qR, CR1, CR3, and CR4 that are responsible for phagocytosis of bacteria *via* C3b/iC3b recognition.[47] Lymphocytes express complement receptor CR2, which is the receptor for C3d and is responsible for antigen presentation on B-lymphocytes and cell adhesion of T-lymphocytes,[48,49] and CR1, which is responsible for capturing, postprocessing and trafficking of C3b-opsonized pathogens. In case of platelets, it is not clear whether they express classical complement receptors. Several reports suggest that C3b-opsonized pathogens could bind to platelets *via* glycoprotein GpIIb/IIIa.[50,51] Another possibility is P-selectin, which can mediate platelet adhesion to immobilized C3b.[52] Interestingly, we observed that many platelets adhere to neutrophils. C3a and C5b-9 activate platelets,[53,54] and activated platelets are prone to form heteroaggregates with leukocytes *via* the platelet P-selectin and the leukocyte P-selectin glycoprotein ligand-1, and/or GpIIa and complement receptor 3.[55,56] Accordingly, the interaction between leukocytes and platelets due to complement-mediated processes could be an interesting and unexpected twist to nanoparticle behavior *in vivo*. To fill this gap of knowledge, we are currently performing studies on the role of the complement receptors in the recognition and uptake.

The consequences of complement activation and subsequent immune recognition by leukocytes and platelets could be far reaching. Uncontrolled complement activation is known to cause inflammation,[4] immune cell activation,[57] increase vascular permeability[58] and even trigger tumor growth.[59,60] That, together with the known ability of neutrophils, eosinophils, monocytes and even platelets to accumulate in pathological sites may play a critical role in pathogenesis of cancer and other disease.[61–64] For instance, neutrophils could contribute to tumor growth through complex processes including elastase and properdin release.[65] The latter may further enhance intratumoral complement activation and accelerate tumor growth by promoting angiogenesis as well the recruitment of immunosuppressive cells.[66] Understanding the nanomaterial-mediated complement activation together with the role of complement in the crosstalk between activated platelets and leukocytes may further unravel the molecular basis of pulmonary hypertension, which is known to occur on infusion of nanomedicines in some individuals.[67] On the other hand, careful exploitation of complement-mediated interception of blood-borne particles by leukocytes could offer better opportunities for delivery of drugs and contrast agents across many biological barriers by leukocyte “hitchhiking”.

CONCLUSIONS

We demonstrated that blood leukocytes internalize iron oxide nanoworms *via* complement-dependent mechanisms in mice and in humans, and showed that hemocompatibility can be improved either by the inhibition of the complement system, and notably the alternative pathway, or by dextran hydrogelation. In view of the ubiquitous role of complement in inflammation and disease, it is critical to further understand mechanisms of complement activation and complement-mediated uptake of nanoparticles in order to design more safe and efficient nanomedicines.

MATERIALS AND METHODS

Materials

All chemical reagents used for nanoparticle synthesis, including iron salts and 15–25-kDa dextran, were purchased from Sigma-Aldrich (St Louis, MO, US). Cell culture media were purchased from Corning Life Sciences. Antidextran DX-1 antibody was purchased from StemCell Technologies (Vancouver, BC, Canada). Goat antimouse and goat antihuman complement C3 polyclonal antibodies were purchased from MP Biomedicals (Solon, OH). Mouse monoclonal antiproperdin antibodies were purchased from Quidel (San Diego, CA). All fluorescent secondary antibodies for immunostaining were from Thermo Fisher Scientific. Copper grids (300 mesh) were purchased from Electron Microscopy Sciences (Hatfield, PA, US). BALB/c mice were bred in an animal vivarium at the University of Colorado Denver Anschutz Medical Campus according to the IACUC approved breeding protocol. The BALB/c breeder mice were purchased from Charles River Laboratories International, Inc. (Wilmington, MA). $C3^{-/-}$ mice (B6;129S4-$C3^{tm1Crr}$/J) were obtained from Dr. Holers and bred in house. C57BL6 mice (Charles River) were used as a control for knockout experiments.

SPIO NWs Preparation and Cross-Linking

NWs were synthesized using a one-pot Molday and MacKenzie[34] precipitation method using dextran, Fe(III) chloride and Fe(II) chloride as described previously.[26] Nanoparticles were filtered through a 0.45-μm filter and stored sterile at 4 °C. Nanoparticles were cross-linked using epichlorohydrin in a two-step harsh cross-linking procedure as described previously.[26] Transmission electron microscopy (TEM) imaging was conducted to visualize the NWs using a FEI Tecnai electron microscope at a 100 kV working voltage. Size was determined using a NanoSight instrument (Malvern Instruments Ltd., Malvern, UK) after diluting 1 mg/mL solution of particles in sterile double distilled water 10 000 times. The data were reported as number weighted mean.

NWs Uptake *In Vitro*

For uptake experiments, blood from nontumor-bearing and 4T1 tumor-bearing mice was obtained by cardiac puncture. Sodium EDTA or heparin anticoagulated blood from healthy male and female volunteers was obtained from Bioreclamation LLC (Baltimore, MD). Sodium EDTA anticoagulated blood from anonymous metastatic triple-negative cancer patient was obtained from Moores UCSD Cancer Center according to an approved

Institutional Research Board (IRB) protocol. Before incubation with SPIO NWs, the blood cells were thoroughly washed with 1% (w/v) BSA-PBS to remove anticoagulated plasma. SPIO NWs were incubated with mouse sera at room temperature for 15 min or human sera at 37C for 30 min. For complement inhibition in human serum, either EDTA (4 mM) or antiproperdin antibody (1:10 dilution) was added to serum for 15 min prior to the addition of SPIO NWs. At the end of incubation, the SPIO NWs-serum mix was added to the washed blood and incubated at 37°C for 1 h. The blood was then washed by centrifugation to remove the NWs, and the cells with internalized SPIO NWs were collected using Miltenyi Biotec Mini MACS magnetic columns. The eluted cells from different groups were suspended in equal amounts of 1% (w/v) BSA-PBS and were concentrated on glass slides using cytospin (Thermo Fisher Scientific). The slides were then fixed with 10% (v/v) formalin in PBS and stained with Hoechst nuclear stain (Thermo Fisher). Main leukocyte types were counted under fluorescent microscope. Leukocyte types nuclear shape has been used to differentiate between lymphocytes (round shape), monocytes (kidney shape), neutrophils (multilobe, segmented shape) and eosinophils (bilobe nucleus connected by a thin bridge).[36] Each experiment yielded 2–3 slides, and on each side, 10–20 random microscopic areas were captured under ×200 magnification. Between 500 and 1000 cells were counted in order to calculate the percentage of each leukocyte type.

Dot Blot C3 Binding Assay

For binding assay of complement C3 in mouse and human serum, SPIO NWs were incubated with serum as described above. At the end of incubation, particles were washed 3 times with 1X PBS by centrifugation at 55 000*g* at room temperature using Beckman Optima TLX ultracentrifuge. The pellets were resuspended in 20 μL PBS, and 2 μL aliquots were applied in triplicate onto a nitrocellulose membrane. The membranes were blocked using 5% (w/w) nonfat dry milk in PBS-T (1 × PBS with 0.1% Tween 20) for 1 h at room temperature, probed with corresponding primary antibodies for 1 h at room temperature, followed by washing the membranes 3 times with PBS-T, and finally 1 h incubation with the corresponding IRDye 800CW-labeled secondary antibodies against the primary antibody species. After immunoblotting, the membranes were visualized using an Odyssey infrared imager (Li-COR Biosciences, Lincoln, NE, US). The integrated dot intensity in the scanned images was quantitatively analyzed using ImageJ software and plotted using Prism 6 software (GraphPad Software, Inc. La Jolla, CA, US).

Nanoparticle Uptake *In Vivo*

NWs were injected as a 0.1 mg bolus *via* tail vein injection into WT and C3KO C57/BL6 mice. Following the injection, blood was collected *via* retro-orbital bleeding at different time points (10 min, 1h and 24 h) using heparin as anticoagulant. Blood was washed, and the cells internalized with SPIO NWs were collected employing Miltenyi MiniMACS magnetic columns and concentrated on slides as described above. The slides were then fixed with 10% (v/v) formalin in PBS and stained to enable differential counting.

Leukocyte Labeling

Peripheral blood was collected from BALB/c mice by cardiac puncture using heparin as anticoagulant. Blood was centrifuged at 2000*g* for 5 min at room temperature, the

supernatant was discarded and red blood cells were lysed with RBC Lysis Buffer Solution (eBioscience, San Diego, USA). Leukocytes were washed 2 times with 1 × DPBS (Corning, Manassas, USA). Leukocytes (1×10^6 cells/mL) were labeled with 10 μM carboxyfluorescein succinimidyl ester CFSE (eBioscience) at room temperature for 8 min. Reaction was blocked with 2% fetal calf serum, and the cells were washed in 1 × DPBS 2 times. Resuspended leukocytes were incubated with 0.1 mg/mL SPIO NWs (preincubated with mouse serum as described above) at 37 °C with gentle shaking for 1 h. SPIO NWs labeled leukocytes were isolated with MiniMACS column; both magnetic and non magnetic fraction were collected. Mice were injected with 0.5–1×10^6 leukocytes in 100 μL PBS *via* intravenous injection. Blood was collected from the periorbital plexus at 1 min, 10 min, 60 min, 240 and 1440 min postinjection and CFSE positive cells were counted with hemocytometer.

Immunofluorescence

The slides were blocked with 10% (v/v) goat serum and incubated with antidextran antibody and either CD11b or CD41antibodies for 1 h at RT. At the end of incubation, slides were washed with 0.1% PBS-T and incubated with goat antimouse Alexa Fluor 488 and goat antirat Alexa Fluor 594 secondary antibodies along with Hoechst to stain the nucleus at room temperature for 1 h. The slides were washed to remove excess antibody and observed under a Nikon inverted microscope (Nikon Eclipse TE300) at 400× magnification. Images were captured using an attached CCD camera and the differential counting was done based on the shape of the nucleus.

Supplementary Material

Refer to Web version on PubMed Central for supplementary material.

Acknowledgments

This study was funded by the University of Colorado Denver startup funding and by 7R21CA167524-3 to D.S. F.C. was supported by the International Postdoctoral Exchange Fellowship Program (2013) funded by China Postdoctoral Council. We would like to thank Drs. T. Anchordoquy and M. Kullberg for useful discussions, and Mr. J. J. Hesson for editing this manuscript.

REFERENCES AND NOTES

1. Grodzinski P, Farrell D. Future Opportunities in Cancer Nanotechnology--Nci Strategic Workshop Report. Cancer Res. 2014; 74:1307–1310. [PubMed: 24413533]
2. Hull LC, Farrell D, Grodzinski P. Highlights of Recent Developments and Trends in Cancer Nanotechnology Research--View from NCI Alliance for Nanotechnology in Cancer. Biotechnol Adv. 2014; 32:666–678. [PubMed: 23948249]
3. Taylor PR, Martinez-Pomares L, Stacey M, Lin HH, Brown GD, Gordon S. Macrophage Receptors and Immune Recognition. Annu Rev Immunol. 2005; 23:901–944. [PubMed: 15771589]
4. Ricklin D, Hajishengallis G, Yang K, Lambris JD. Complement: A Key System for Immune Surveillance and Homeostasis. Nat Immunol. 2010; 11:785–797. [PubMed: 20720586]
5. Helmy KY, Katschke KJ Jr, Gorgani NN, Kljavin NM, Elliott JM, Diehl L, Scales SJ, Ghilardi N, van Lookeren Campagne M. Crig: A Macrophage Complement Receptor Required for Phagocytosis of Circulating Pathogens. Cell. 2006; 124:915–927. [PubMed: 16530040]

6. Peng Q, Li K, Sacks SH, Zhou W. The Role of Anaphylatoxins C3a and C5a in Regulating Innate and Adaptive Immune Responses. Inflammation Allergy: Drug Targets. 2009; 8:236–246. [PubMed: 19601884]
7. Moghimi SM, Farhangrazi ZS. Nanomedicine and the Complement Paradigm. Nanomedicine. 2013; 9:458–460. [PubMed: 23499667]
8. Andersen AJ, Hashemi SH, Andresen TL, Hunter AC, Moghimi SM. Complement: Alive and Kicking Nanomedicines. J Biomed Nanotechnol. 2009; 5:364–372. [PubMed: 20055082]
9. Andersen AJ, Robinson JT, Dai H, Hunter AC, Andresen TL, Moghimi SM. Single-Walled Carbon Nanotube Surface Control of Complement Recognition and Activation. ACS Nano. 2013; 7:1108–1119. [PubMed: 23301860]
10. Wang X, Ishida T, Kiwada H. Anti-Peg IgM Elicited by Injection of Liposomes is Involved in the Enhanced Blood Clearance of a Subsequent Dose of Pegylated Liposomes. J Controlled Release. 2007; 119:236–244.
11. Auguste DT, Prud'homme RK, Ahl PL, Meers P, Kohn J. Association of Hydrophobically-Modified Poly(Ethylene Glycol) with Fusogenic Liposomes. Biochim Biophys Acta, Biomembr. 2003; 1616:184–195.
12. Hamad I, Hunter AC, Moghimi SM. Complement Monitoring of Pluronic 127 Gel and Micelles: Suppression of Copolymer-Mediated Complement Activation by Elevated Serum Levels of Hdl, Ldl, and Apolipoproteins Ai and B-100. J Controlled Release. 2013; 170:167–174.
13. Devine DV, Wong K, Serrano K, Chonn A, Cullis PR. Liposome-Complement Interactions in Rat Serum: Implications for Liposome Survival Studies. Biochim Biophys Acta, Biomembr. 1994; 1191:43–51.
14. Borchard G, Kreuter J. The Role of Serum Complement on the Organ Distribution of Intravenously Administered Poly (Methyl Methacrylate) Nanoparticles: Effects of Pre-Coating with Plasma and with Serum Complement. Pharm Res. 1996; 13:1055–1058. [PubMed: 8842044]
15. Dobrovolskaia MA, Patri AK, Zheng J, Clogston JD, Ayub N, Aggarwal P, Neun BW, Hall JB, McNeil SE. Interaction of Colloidal Gold Nanoparticles with Human Blood: Effects on Particle Size and Analysis of Plasma Protein Binding Profiles. Nanomedicine. 2008; 5:106–117. [PubMed: 19071065]
16. Szebeni J. Complement Activation-Related Pseudoallergy: A New Class of Drug-Induced Acute Immune Toxicity. Toxicology. 2005; 216:106–121. [PubMed: 16140450]
17. Pedersen MB, Zhou X, Larsen EK, Sorensen US, Kjems J, Nygaard JV, Nyengaard JR, Meyer RL, Boesen T, Vorup-Jensen T. Curvature of Synthetic and Natural Surfaces Is an Important Target Feature in Classical Pathway Complement Activation. J Immunol. 2010; 184:1931–1945. [PubMed: 20053940]
18. Peracchia MT, Vauthier C, Passirani C, Couvreur P, Labarre D. Complement Consumption by Poly(Ethylene Glycol) in Different Conformations Chemically Coupled to Poly(Isobutyl 2-Cyanoacrylate) Nanoparticles. Life Sci. 1997; 61:749–761. [PubMed: 9252249]
19. Pham CT, Mitchell LM, Huang JL, Lubniewski CM, Schall OF, Killgore JK, Pan D, Wickline SA, Lanza GM, Hourcade DE. Variable Antibody-Dependent Activation of Complement by Functionalized Phospholipid Nanoparticle Surfaces. J Biol Chem. 2011; 286:123–130. [PubMed: 21047788]
20. Al-Hanbali O, Rutt KJ, Sarker DK, Hunter AC, Moghimi SM. Concentration Dependent Structural Ordering of Poloxamine 908 on Polystyrene Nanoparticles and Their Modulatory Role on Complement Consumption. J Nanosci Nanotechnol. 2006; 6:3126–3133. [PubMed: 17048527]
21. Moghimi SM, Hamad I, Andresen TL, Jorgensen K, Szebeni J. Methylation of the Phosphate Oxygen Moiety of Phospholipid-Methoxy(Polyethylene Glycol) Conjugate Prevents Pegylated Liposome-Mediated Complement Activation and Anaphylatoxin Production. FASEB J. 2006; 20:2591–2593. [PubMed: 17065229]
22. Salvador-Morales C, Zhang L, Langer R, Farokhzad OC. Immunocompatibility Properties of Lipid-Polymer Hybrid Nanoparticles with Heterogeneous Surface Functional Groups. Biomaterials. 2009; 30:2231–2240. [PubMed: 19167749]
23. Moore A, Weissleder R, Bogdanov A Jr. Uptake of Dextran-Coated Monocrystalline Iron Oxides in Tumor Cells and Macrophages. J Magn Reson Imaging. 1997; 7:1140–1145. [PubMed: 9400860]

24. Figuerola A, Di Corato R, Manna L, Pellegrino T. From Iron Oxide Nanoparticles Towards Advanced Iron-Based Inorganic Materials Designed for Biomedical Applications. Pharmacol Res. 2010; 62:126–143. [PubMed: 20044004]
25. Park JH, von Maltzahn G, Zhang L, Schwartz MP, Ruoslahti E, Bhatia S, Sailor MJ. Magnetic Iron Oxide Nanoworms for Tumor Targeting and Imaging. Adv Mater. 2008; 20:1630–1635. [PubMed: 21687830]
26. Wang G, Inturi S, Serkova NJ, Merkulov S, McCrae K, Russek SE, Banda NK, Simberg D. High-Relaxivity Superparamagnetic Iron Oxide Nanoworms with Decreased Immune Recognition and Long-Circulating Properties. ACS Nano. 2014; 8:12437–12449. [PubMed: 25419856]
27. Karmali PP, Chao Y, Park JH, Sailor MJ, Ruoslahti E, Esener SC, Simberg D. Different Effect of Hydrogelation on Antifouling and Circulation Properties of Dextran-Iron Oxide Nanoparticles. Mol Pharmaceutics. 2012; 9:539–545.
28. Banda NK, Mehta G, Chao Y, Wang G, Inturi S, Fossati-Jimack L, Botto M, Wu L, Moghimi S, Simberg D. Mechanisms of Complement Activation by Dextran-Coated Superparamagnetic Iron Oxide (SPIO) Nanoworms in Mouse *Versus* Human Serum. Part Fibre Toxicol. 2014; 11:64–73. [PubMed: 25425420]
29. Zamboni WC, Maruca LJ, Strychor S, Zamboni BA, Ramalingam S, Edwards RP, Kim J, Bang Y, Lee H, Friedland DM, et al. Bidirectional Pharmacodynamic Interaction between Pegylated Liposomal Ckd-602 (S-Ckd602) and Monocytes in Patients with Refractory Solid Tumors. J Liposome Res. 2011; 21:158–165. [PubMed: 20626314]
30. Wu YJ, Muldoon LL, Varallyay C, Markwardt S, Jones RE, Neuwelt EA. *In vivo* Leukocyte Labeling with Intravenous Ferumoxides/Protamine Sulfate Complex and *in vitro* Characterization for Cellular Magnetic Resonance Imaging. Am J Physiol Cell Physiol. 2007; 293:C1698–1708. [PubMed: 17898131]
31. Leroux JC, Gravel P, Balant L, Volet B, Anner BM, Allemann E, Doelker E, Gurny R. Internalization of Poly(D,L-Lactic Acid) Nanoparticles by Isolated Human Leukocytes and Analysis of Plasma Proteins Adsorbed onto the Particles. J Biomed Mater Res. 1994; 28:471–481. [PubMed: 8006052]
32. Zambaux MF, Faivre-Fiorina B, Bonneau F, Marchal S, Merlin JL, Dellacherie E, Labrude P, Vigneron C. Involvement of Neutrophilic Granulocytes in the Uptake of Biodegradable Non-Stealth and Stealth Nanoparticles in Guinea Pig. Biomaterials. 2000; 21:975–980. [PubMed: 10768748]
33. Bartneck M, Keul HA, Singh S, Czaja K, Bornemann J, Bockstaller M, Moeller M, Zwadlo-Klarwasser G, Groll J. Rapid Uptake of Gold Nanorods by Primary Human Blood Phagocytes and Immunomodulatory Effects of Surface Chemistry. ACS Nano. 2010; 4:3073–3086. [PubMed: 20507158]
34. Molday RS, MacKenzie D. Immunospecific Ferromagnetic Iron-Dextran Reagents for the Labeling and Magnetic Separation of Cells. J Immunol Methods. 1982; 52:353–367. [PubMed: 7130710]
35. Gerges N, Rak J, Jabado N. New Technologies for the Detection of Circulating Tumour Cells. Br Med Bull. 2010; 94:49–64. [PubMed: 20418405]
36. Estridge, BH.; Reynolds, AP. Basic Clinical Laboratory Techniques. Cengage Learning; Independence, KY: 2012. Normal Cell Morphology; p. 291-293.
37. Hiremath P, Bannigidad P, Geeta S. Automated Identification and Classification of White Blood Cells (Leukocytes) in Digital Microscopic Images. Int J Comput Appl. 2010:59–63. Special issue on “Recent Trends in Image Processing and Pattern Recognition” RTIPPR.
38. Putzu L, Caocci G, Di Ruberto C. Leucocyte Classification for Leukaemia Detection Using Image Processing Techniques. Artif Intell Med. 2014; 62:179–191. [PubMed: 25241903]
39. Aslakson CJ, Miller FR. Selective Events in the Metastatic Process Defined by Analysis of the Sequential Dissemination of Subpopulations of a Mouse Mammary Tumor. Cancer Res. 1992; 52:1399–1405. [PubMed: 1540948]
40. Becker HM, Chen M, Hay JB, Cybulsky MI. Tracking of Leukocyte Recruitment into Tissues of Mice by *in situ* Labeling of Blood Cells with the Fluorescent Dye Cfda Se. J Immunol Methods. 2004; 286:69–78. [PubMed: 15087222]

41. Asquith B, Debacq C, Florins A, Gillet N, Sanchez-Alcaraz T, Mosley A, Willems L. Quantifying Lymphocyte Kinetics *in vivo* Using Carboxyfluorescein Diacetate Succinimidyl Ester (Cfse). Proc R Soc London, Ser B. 2006; 273:1165–1171.
42. Kemper C, Atkinson JP, Hourcade DE. Properdin: Emerging Roles of a Pattern-Recognition Molecule. Annu Rev Immunol. 2010; 28:131–155. [PubMed: 19947883]
43. Gupta-Bansal R, Parent JB, Brunden KR. Inhibition of Complement Alternative Pathway Function with Anti-Properdin Monoclonal Antibodies. Mol Immunol. 2000; 37:191–201. [PubMed: 10930626]
44. Park JH, von Maltzahn G, Zhang L, Derfus AM, Simberg D, Harris TJ, Ruoslahti E, Bhatia SN, Sailor MJ. Systematic Surface Engineering of Magnetic Nanoworms for *in vivo* Tumor Targeting. Small. 2009; 5:694–700. [PubMed: 19263431]
45. Wang G, Inturi S, Serkova NJ, Merkulov S, McCrae K, Russek SE, Banda NK, Simberg D. High-Relaxivity Superparamagnetic Iron Oxide Nanoworms with Minimal Immune Recognition and Long-Circulating Properties. ACS Nano. 2014; 7:4289–4298.
46. Dos Santos N, Allen C, Doppen AM, Anantha M, Cox KA, Gallagher RC, Karlsson G, Edwards K, Kenner G, Samuels L, et al. Influence of Poly(Ethylene Glycol) Grafting Density and Polymer Length on Liposomes: Relating Plasma Circulation Lifetimes to Protein Binding. Biochim Biophys Acta, Biomembr. 2007; 1768:1367–1377.
47. Sengelov H. Complement Receptors in Neutrophils. Crit Rev Immunol. 1995; 15:107–131. [PubMed: 8573284]
48. Heyman B, Wiersma EJ, Kinoshita T. *In vivo* Inhibition of the Antibody Response by a Complement Receptor-Specific Monoclonal Antibody. J Exp Med. 1990; 172:665–668. [PubMed: 1695671]
49. Levy E, Ambrus J, Kahl L, Molina H, Tung K, Holers VM. T Lymphocyte Expression of Complement Receptor 2 (Cr2/Cd21): A Role in Adhesive Cell-Cell Interactions and Dysregulation in a Patient with Systemic Lupus Erythematosus (Sle). Clin Exp Immunol. 1992; 90:235–244. [PubMed: 1424280]
50. Verschoor A, Neuenhahn M, Navarini AA, Graef P, Plaumann A, Seidlmeier A, Nieswandt B, Massberg S, Zinkernagel RM, Hengartner H, et al. A Platelet-Mediated System for Shuttling Blood-Borne Bacteria to Cd8alpha+Dendritic Cells Depends on Glycoprotein Gpib and Complement C3. Nat Immunol. 2011; 12:1194–1201. [PubMed: 22037602]
51. Fitzgerald JR, Foster TJ, Cox D. The Interaction of Bacterial Pathogens with Platelets. Nat Rev Microbiol. 2006; 4:445–457. [PubMed: 16710325]
52. Del Conde I, Cruz MA, Zhang H, Lopez JA, Afshar-Kharghan V. Platelet Activation Leads to Activation and Propagation of the Complement System. J Exp Med. 2005; 201:871–879. [PubMed: 15781579]
53. Wiedmer T, Sims PJ. Effect of Complement Proteins C5b-9 on Blood Platelets. Evidence for Reversible Depolarization of Membrane Potential. J Biol Chem. 1985; 260:8014–8019. [PubMed: 4008487]
54. Polley MJ, Nachman RL. Human Platelet Activation by C3a and C3a Des-Arg. J Exp Med. 1983; 158:603–615. [PubMed: 6604123]
55. Li N, Hu H, Lindqvist M, Wikstrom-Jonsson E, Goodall AH, Hjemdahl P. Platelet-Leukocyte Cross Talk in Whole Blood. Arterioscler, Thromb, Vasc Biol. 2000; 20:2702–2708. [PubMed: 11116075]
56. Rinder CS, Rinder HM, Smith BR, Fitch JC, Smith MJ, Tracey JB, Matis LA, Squinto SP, Rollins SA. Blockade of C5a and C5b-9 Generation Inhibits Leukocyte and Platelet Activation During Extracorporeal Circulation. J Clin Invest. 1995; 96:1564–1572. [PubMed: 7657827]
57. Volk LD, Flister MJ, Bivens CM, Stutzman A, Desai N, Trieu V, Ran S. Nab-Paclitaxel Efficacy in the Orthotopic Model of Human Breast Cancer Is Significantly Enhanced by Concurrent Anti-Vascular Endothelial Growth Factor a Therapy. Neoplasia. 2008; 10:613–623. [PubMed: 18516298]
58. Williams TJ, Jose PJ. Mediation of Increased Vascular Permeability after Complement Activation. Histamine-Independent Action of Rabbit C5a. J Exp Med. 1981; 153:136–153. [PubMed: 6161204]

59. Rutkowski MJ, Sughrue ME, Kane AJ, Mills SA, Parsa AT. Cancer and the Complement Cascade. Mol Cancer Res. 2010; 8:1453–1465. [PubMed: 20870736]

60. Moghimi SM. Cancer Nanomedicine and the Complement System Activation Paradigm: Anaphylaxis and Tumour Growth. J Controlled Release. 2014; 190:556–562.

61. Bambace NM, Holmes CE. The Platelet Contribution to Cancer Progression. J Thromb Haemostasis. 2011; 9:237–249. [PubMed: 21040448]

62. Davis BP, Rothenberg ME. Eosinophils and Cancer. Cancer Immunol Res. 2014; 2:1–8. [PubMed: 24778159]

63. Cools-Lartigue J, Spicer J, McDonald B, Gowing S, Chow S, Giannias B, Bourdeau F, Kubes P, Ferri L. Neutrophil Extracellular Traps Sequester Circulating Tumor Cells and Promote Metastasis. J Clin Invest. 2013; 123:3446–3458.

64. Spicer JD, McDonald B, Cools-Lartigue JJ, Chow SC, Giannias B, Kubes P, Ferri LE. Neutrophils Promote Liver Metastasis *Via* Mac-1-Mediated Interactions with Circulating Tumor Cells. Cancer Res. 2012; 72:3919–3927. [PubMed: 22751466]

65. Wirthmueller U, Dewald B, Thelen M, Schafer MK, Stover C, Whaley K, North J, Eggleton P, Reid KB, Schwaeble WJ. Properdin, a Positive Regulator of Complement Activation, Is Released from Secondary Granules of Stimulated Peripheral Blood Neutrophils. J Immunol. 1997; 158:4444–4451. [PubMed: 9127010]

66. Loveland BE, Cebon J. Cancer Exploiting Complement: A Clue or an Exception? Nat Immunol. 2008; 9:1205–1206. [PubMed: 18936777]

67. Moghimi SM, Farhangrazi ZS. Just So Stories: The Random Acts of Anti-Cancer Nanomedicine Performance. Nanomedicine. 2014; 10:1661–1666. [PubMed: 24832960]

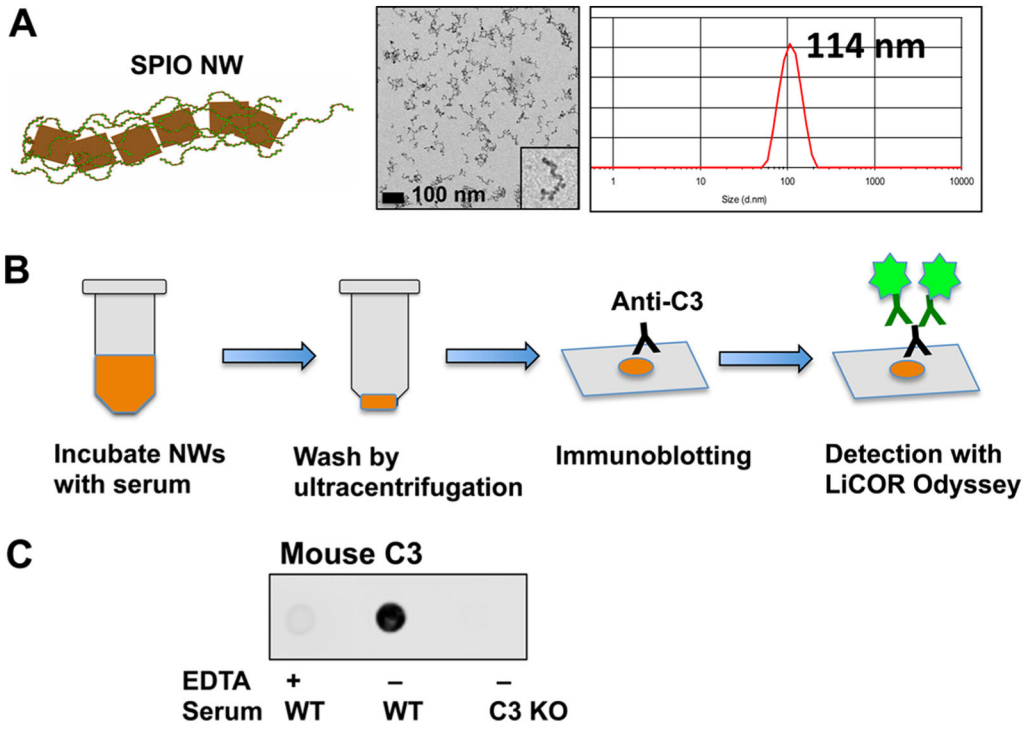

Figure 1.

Characterization of SPIO NWs and complement activation in sera: (A) Size of SPIO NWs as determined with transmission electron microscopy and dynamic light scattering. (B) Dot blot assay of complement C3 deposition on NWs. Following incubation with mouse serum, NWs were washed and analyzed for complement C3 binding as described previously.[26] (C) The deposition was absent in 4 mM EDTA supplemented wild-type (WT) serum and in C3-KO serum.

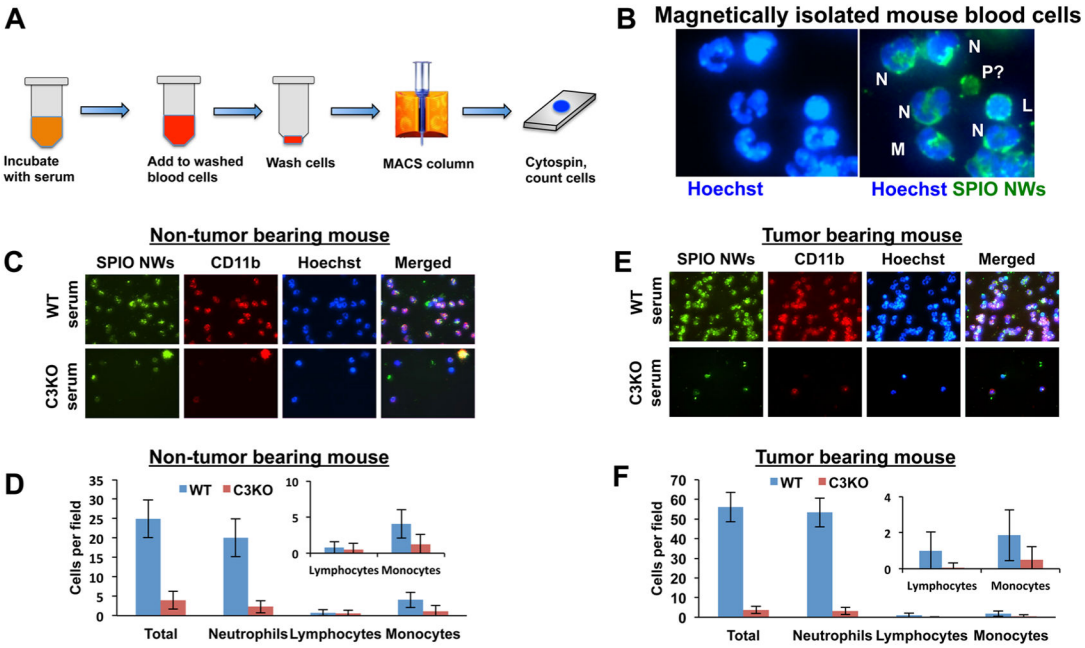

Figure 2.

Complement dependent uptake of SPIO NWs *in vitro*: (A) Workflow of *in vitro* uptake experiments. (B) Magnetically isolated blood cells were identified by the nuclear shape. N = neutrophil; M = monocyte; L = lymphocyte; P = platelet, (C,D) Uptake of SPIO NWs preincubated in normal (WT) or C3-deficient (C3KO) sera by leukocytes derived from nontumor bearing C57/BL6J mice. Cells were stained with antidextran antibody (SPIO NWs, green) and anti-CD11b antibody (complement receptor CR3, red). (E,F) Uptake of SPIO NWs by leukocytes derived from 4T1 tumor-bearing BALB/c mice. In both normal and tumor-bearing mice, leukocyte uptake was highly dependent on C3. Neutrophils were the predominant cells that internalized SPIO NWs in normal and tumor-bearing mice. One representative microscope field out of 10–15 is shown. Each experiment was repeated at least 3 times. All colors were enhanced by ImageJ software to the same extent for visual clarity.

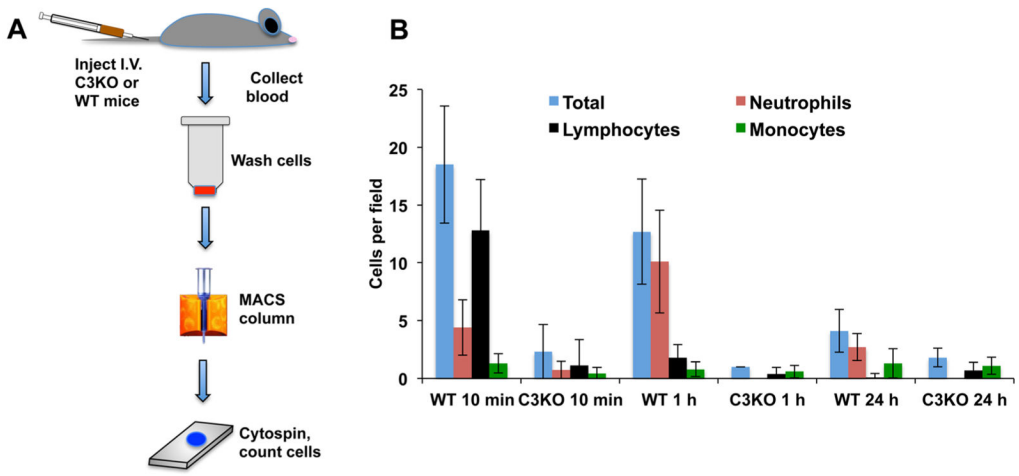

Figure 3.

Complement dependent uptake of SPIO NWs by mouse leukocytes *in vivo*. SPIO NWs were injected into C3-deficient and control mice. (A) Workflow of *in vivo* experiments. (B) Results from one representative *in vivo* experiment (total $N = 4$) is shown. Cells were enumerated by their nuclear shape as described in Figure 2. The uptake by all cell types was decreased in C3 deficient mice.

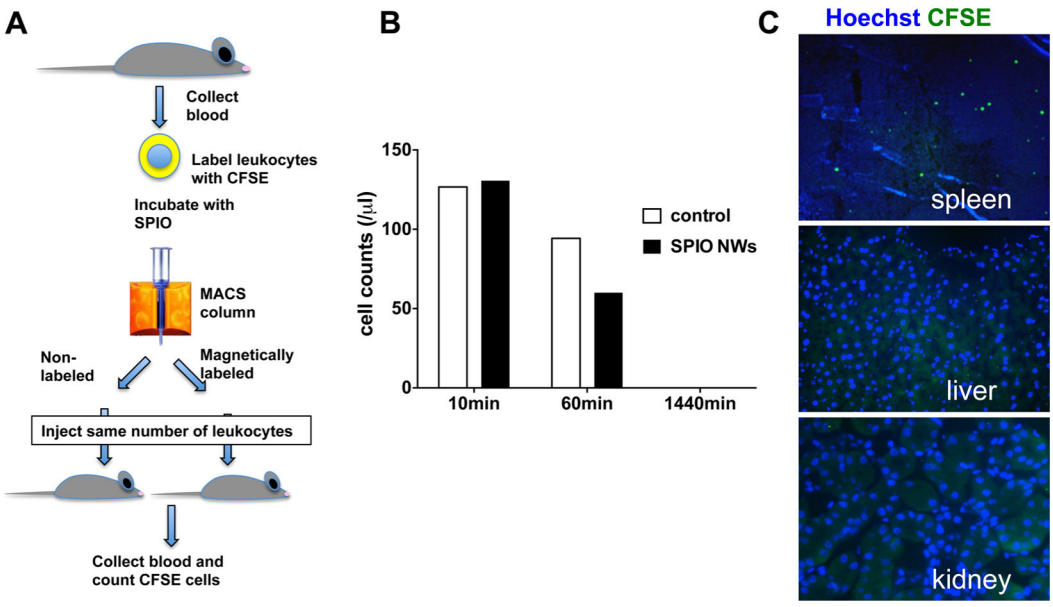

Figure 4.

Circulation and organ distribution of magnetically labeled leukocytes: (A) Workflow of *ex vivo* cell labeling of leukocytes with CFSE or CFSE and SPIO NWs (full description in Materials and Methods). Cells were injected into mice at 0.5×10^6 cells per mouse. (B) Levels of the circulating CFSE-labeled cells measured by sampling blood and counting the fluorescent cells under microscope. Cells in both groups disappeared from circulation at 24 h postinjection. Data from a representative experiment (out of 3) are shown. (C) CFSE/SPIO NWs labeled cells accumulated in the spleen, but not in the liver or kidneys. Control (nonmagnetically labeled cells) cells showed similar distribution (not shown).

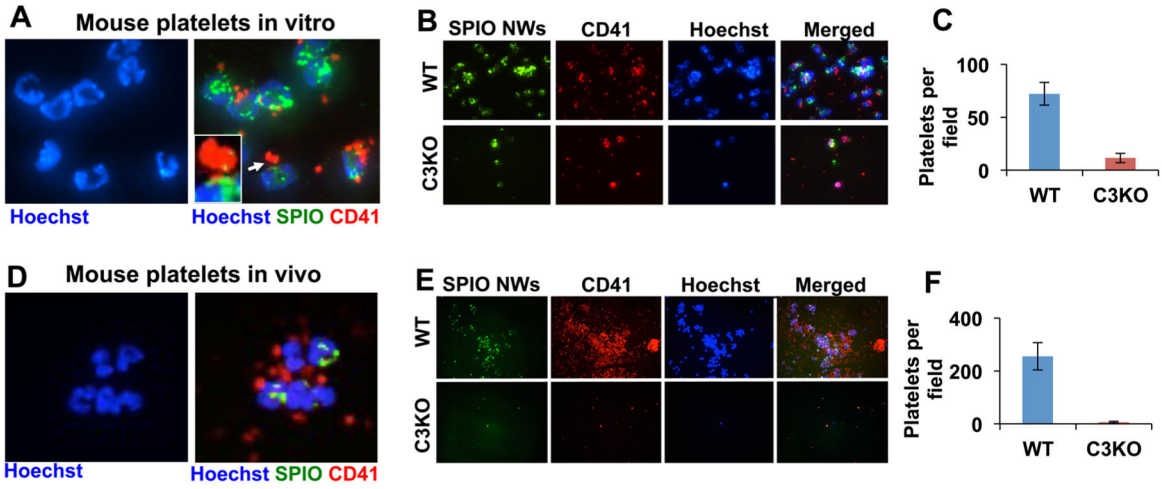

Figure 5.

Complement dependent binding of SPIO NWs to mouse platelets *in vitro* and *in vivo*: SPIO NWs were incubated with washed mouse blood as described in Figure 1A, or injected into mice as described in Figure 2A. The magnetically isolated cells were stained for dextran on SPIO NWs (green) and CD41 (platelet marker). Platelets were counted based on the CD41 staining. (A–C) Platelets became magnetically labeled after incubation with SPIO NWs in normal serum but not in C3KO serum. (D–F) Platelet became magnetically labeled after injection into normal mice but not C3 KO mice. In both *in vitro* and *in vivo* experiments, there were solitary scattered platelets as well as platelets bound to the cells surface. Images show representative microscopical fields, out of 10 counted. The experiments were repeated at least 2 times.

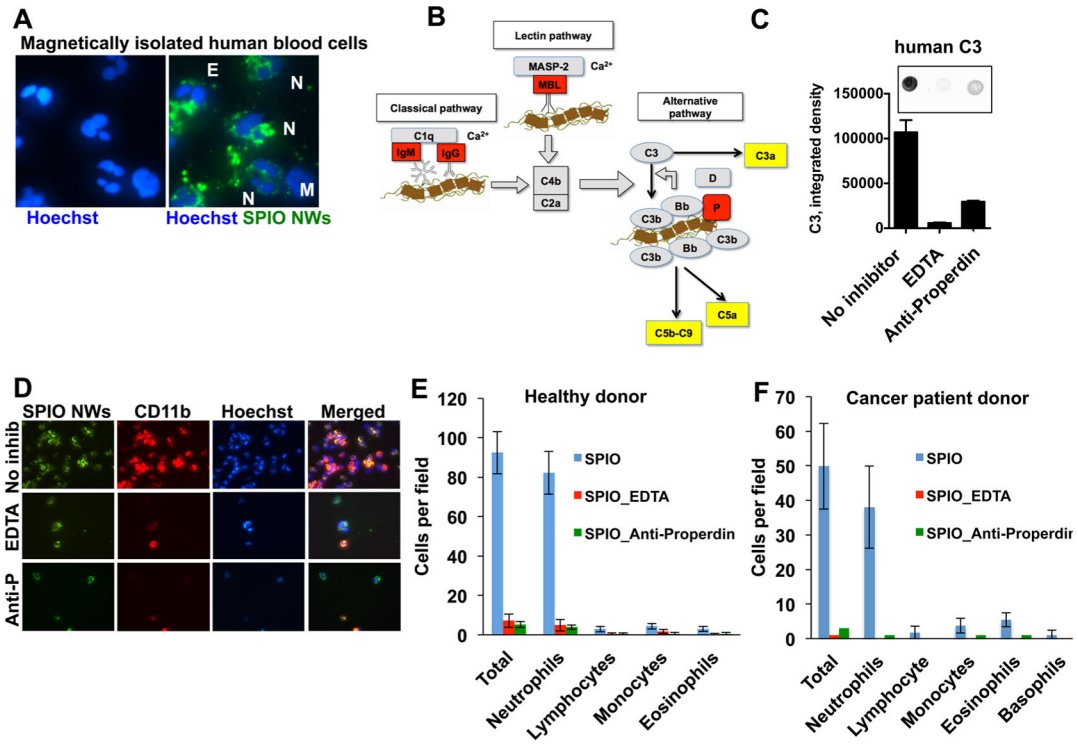

Figure 6.

Complement dependent uptake of SPIO NW in human serum: SPIO NWs were incubated with human blood cells and isolated as described in Figure 1A. (A) A representative microscopic field (high magnification) shows leukocytes magnetically labeled with SPIO NWs. E = eosinophil, N = neutrophil; M = monocyte. (B) Activation of complement in human sera by NWs is mostly *via* the alternative pathway.[28] Properdin (P) is a serum factors that stabilizes the AP convertase C3bBb. (C) Complement C3 deposition in human serum was inhibited by EDTA or anti-Properdin Ab. (D,E) Complement dependent uptake by leukocytes from blood of a healthy donor. (F) Complement dependent uptake by leukocytes from blood of a breast cancer patient.

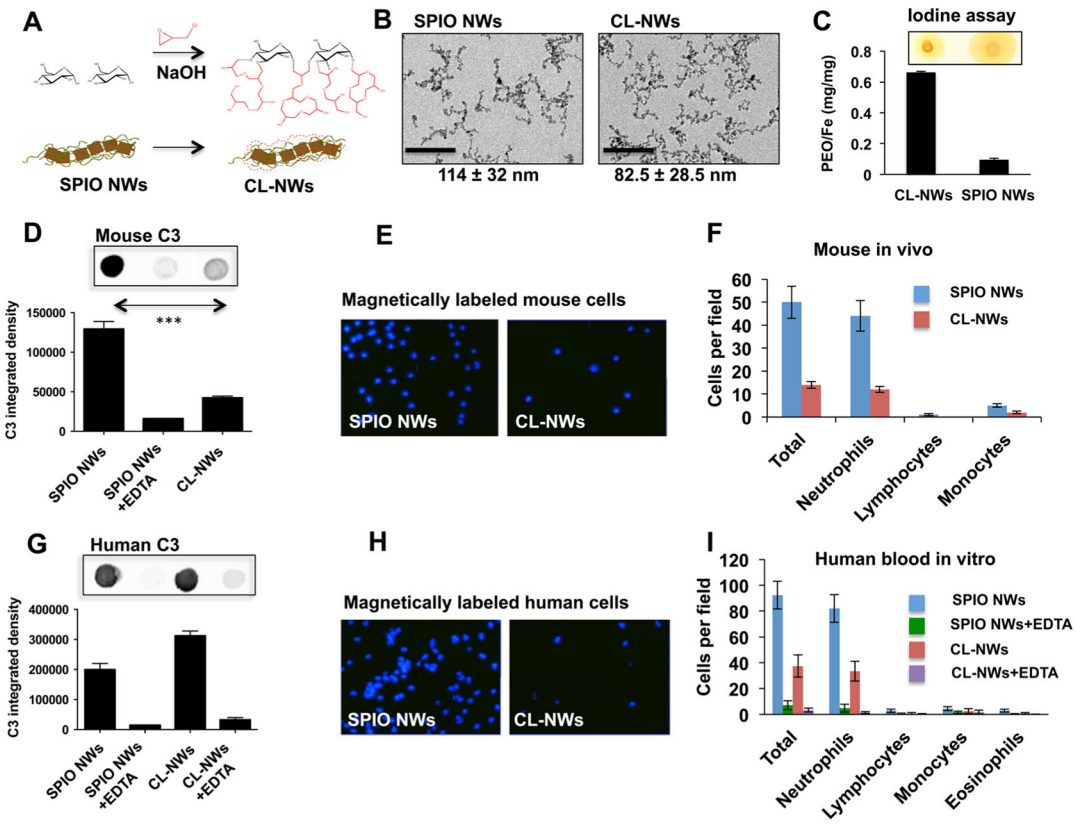

Figure 7.

Cross-linking of dextran shell decreases leukocyte uptake in mice and humans: (A) SPIO NWs were cross-linked with epichlorohydrin in order to obtain hydrogel coated CL-NWs. (B) Size and shape of nanoparticles was not significantly affected by the cross-linking. (C) Formation of cross-linked poly(2-hydroxypropyl ether) hydrogel measured with iodine that reacts with poly(ethylene oxide) (PEO). The assay was performed as described before[26] using PEG 10 kDa for generation of a standard curve. (D) Cross-linking led to a significant ($p < 0.0001$, $n = 3$, t test) decrease in C3 opsonization. (E,F) Injection of cross-linked particles resulted in a decrease in the number of magnetically labeled leukocytes in normal C57/BL6 mice, as compared to non cross-linked SPIO NWs. The experiment was repeated 3 times. (G) Cross-linking did not decrease or even increased the level of C3 opsonization in human serum. (H,I) Incubation of cross-linked particles with human leukocytes (as in Figure 6) resulted in over 60% decrease in the number of magnetically labeled leukocytes. The effect of cross-linking on the uptake was variable among different donors, and inhibition efficiencies ranging from 30% to 70% were observed (not shown). EDTA inhibited the residual uptake of CL-NWs, suggesting the involvement of complement.